Geophysical and geological interpretation of regional structures within the Precambrian Kautokeino Greenstone Belt, Finnmark, North Norway.

ODLEIV OLESEN & ARNE SOLLI

Olesen, O. & Solli, A. 1985: Geophysical and geological interpretation of regional structures within the Precambrian Kautokeino Greenstone Belt, Finnmark, North Norway. *Nor. geol. unders. Bull. 403,* 119-129.

The Kautokeino Greenstone Belt comprises a synclinorium of volcano-sedimentary rocks. This sequence of Early Proterozoic age is situated between two culminations of gneisses. Large areas of the belt have been mapped in detail (1:50,000) and petrophysical properties of about 1150 rock samples have been measured. Geophysical interpretations based on aeromagnetic and gravlmetric maps have been made. The aeromagnetic interpretation includes a magnetic dislocation map showing three directions of dislocation maxima (NNW, N, NE). From an interpretation of magnetic structures showing patterns, contacts and magnetization levels, the basement and intrusions can be separated from the supracrustals, primary layering in supracrustals can be seen, and the boundaries between rock units can be located. The gravity interpretation includes model calculations along four profiles. The profiles show alternating culminations and depressions within the greenstone belt with maximum depths up to 6km. By combining a magnetic interpretation map and a gravity anomaly map a three-dimensional analysis can be made. Anticlines and synclines in the greenstone belt emerge clearly on this map. It is concluded that most of the deformation is caused by gravitational tectonics.

O. Olesen & A. Solli, Geological Survey of Norway, P.O. Box 3006, N-7001 Trondheim, Norway.

Introduction

In 1980 the Geological Survey of Norway started an investigation programme for the mineral resources in Finnmark (The Finnmark Programme). The programme first concentrated on Finnmarksvidda, which is an area of Precambrian rocks heavily covered by glacial drift. To help produce reliable geological maps from the area, the necessity of a careful geophysical investigation was early realised, and this has resulted in Finnmarksvidda now being one of the best covered areas in Norway with respect to gravity and low-altitude aeromagnetic measurements. The geophysical interpretation not only helps to locate the boundaries between rock units in covered terrains, but also gives information about faults and fault-zones, dip of the rocks and depths of the units. We will here present some of the regional data from the Kautokeino Greenstone Belt (Plate 1). The interpretations are based on aeromagnetic and gravimetric maps combined with petrophysical measurements on rocks and geological mapping. The interpretation of the aeromagnetic maps includes an analysis of magnetic dislocations and an analysis of magnetic pattern, contacts, magnetization levels and rough dip estimations. The gravimetric interpretations involve model calculations along profiles.

The geological mapping carried out by the Geological Survey of Norway has concentrated mainly on the northern part of Plate 1, where a profile across the greenstone belt, embracing the three geological maps Masi, Mollejus and Čarajav'ri (scale 1:50,000), has been made (Solli 1984a,b, Sandstad 1985). Much of the detailed geophysical interpretations are included in these maps.

Geological setting

The Kautokeino Greenstone Belt is a c. 40km-wide belt of volcano-sedimentary rocks of Early Proterozoic age. Several aspects of its geology are treated elsewhere in this volume (see e.g. Siedlecka et al. 1985, Krill et al. 1985, Olsen & Nilsen 1985), only a short summary of the main features of the geology will be given here.

The geological map (Plate 1) is in the northern areas based on published maps by Solli (1984a,b) and Sandstad (1985). In other areas the geology is partly based on published maps by Olsen (1984a,b,c, 1985) and Fareth et al. (1977). When compiling the map we have emphasized our geophysical interpretations.

As seen from Plate 1 the general structural trend for the belt is NNW-SSE. Generally both the bedding and the foliation are steep but to the northeast the dip flattens out, wrapping around the Jer'gul Gneiss Complex. Deformation and metamorphism are low in the central parts and increase towards the gneiss complexes. The greenstone belt is bordered by the Rai'sædno Gneiss Complex and the Jer'gul Gneiss Complex to the west and east, respectively (Plate 1). These are thought to be at least partly of Archaean age and form the basement for the greenstone belt. However, no clear depositional contact between the gneisses and the supracrustals has been found. The contacts are either fault-bounded, or what is usually the case obliterated by younger felsic intrusions. As seen from Plate 1 the western parts of the Jer'gul Gneiss Complex are totally dominated by granodioritic and granitic intrusions. To the south the greenstone belt is intruded by a rather homogeneous quartz monzonite.

The oldest rock unit of the Kautokeino Greenstone Belt is the Gål'denvarri Formation (Solli 1983), which consists of mafic volcanic rocks metamorphosed in amphibolite facies. It has only been found at the eastern margin of the greenstone belt. The gravimetric interpretations do not support a wide extension westward beneath the younger Masi Formation because the Bouguer gravity is very low where the latter occurs in antiformal structures within the greenstone belt.

Above the Gål'denvarri Formation lies the Masi Formation with a supposed angular unconformity. This formation consists of quartzitic rocks. It is found mainly in the eastern part of the greenstone belt, but it also occurs in dome structures in the southern central part.

The main part of the greenstone belt is occupied by the Čas'kejas, Suoluvuobmi and Lik'ča Formations (Siedlecka et al. 1985) which consist mainly of basic volcanites. According to Torske (1977) and Bergh & Torske (1984) the volcanites are formed in a rift zone. They are metamorphosed to amphibolites and greenstones; in Plate 1 this distribution is shown rather than the lithostratigraphic formations. This is done mainly because these data are used in the gravity models.

The volcanites are dominated by basic tuff and tuffites, but basaltic lavas and concordant diabases are also present. Sediments, mainly mica schists, occur fairly commonly in the volcanites, but only in the Suoluvuobmi Formation to the northeast do they make up a considerable portion of the rocks. The wide distribution of the sediments here is mainly due to the flat-lying structures.

The youngest rocks of the greenstone belt are found in the central northern parts. Here it can be demonstrated that the volcanism in the Čas'kejas Formation gradually decreases and that the formation is concordantly overlain by pelites (Bik'kacåkka Fm.) and sandstones (Čaravarri Fm.; Sandstad 1985). This latter formation is about 4-5km thick and is cut on its eastern side by a NNW-SSE-trending fault with a vertical displacement of several kilometres. Brecciation is common both in this and in other directions in the greenstone belt. In the northeastern parts of the area intrusions of albite-diabases are related to NE-SW-trending fault zones. The albite-diabases have a high magnetite content giving a distinct banded anomaly pattern on aeromagnetic maps (Plate 2).

To the northwest mudstones of the Late Proterozoic/Early Cambrian Dividal Group unconformably overlies the greenstone belt. Above this are the Caledonian nappes which in this area consist mainly of feldspathic metasandstones.

Physical properties of the rocks

About 1150 rock samples collected mainly during geological mapping in 1973-74 and 1980-84 have been measured with respect to density and magnetic susceptibility. The results for the main rock units are shown in Table 1. The measurements are grouped so that it is possible to compare different rock units and rock types. In Plate 4 the density data are portrayed in map form. The density values and the sample sites are indicated by coloured 1·1km cells and black dots, respectively. In cells with more than one sample an average value is shown. To show the sample site distribution and the density variation within the different rock units the geological boundaries from Plate 1 are indicated. In Plate 8 the frequency distributions of the most common rock types are presented. The density is determined as wet bulk density with an accuracy of about $10 kg/m^3$. The susceptibility is measured using the natural frequency method with a relative error of 5% and a resolution of about $1 \cdot 10^{-4}$SI.

The rocks in the basement, mostly gneisses and granites, have a predominant low density, but some amphibolites and gabbros with high

Table 1
Physical properties of rocks and rock-units; a,b,c denote total sample, low magnetic fraction, high magnetic fraction, respectively. Units are in SI.
The standard deviation of susceptibility is expressed in decades. Susceptibility values have logarithmic mean values.
1) Mean density of $2.67 \cdot 10^3$ kg/m³ used in the model calculations.

ROCK UNIT/TYPE	NO.	SUSCEPTIBILITY			DENSITY (10^3 kg/m³)		Density adapted for gravity model
		Range	Mean	St.dev.	Range	Mean±st.dev.	
RAI'SÆDNO GNEISS COMPLEX							
Gneiss a	34	.00003- .14184	.00173	1.07032	2.550-3.070	2.711±0.143	
Gneiss b	20		.00027	.49743			
Gneiss c	14		.02440	.42465			2.68 1)
Granite	30	.00004- .01912	.00039	.78839	2.560-2.860	2.636±0.055	
Amphibolite	8	.00071- .08387	.00414	.74701	2.810-3.010	2.900±0.069	
Quartz monzonite	10	.00039- .02450	.01295	.51191	2.720-2.820	2.757±0.026	2.75
JER'GUL GNEISS COMPLEX							
Gneiss	13	.00007- .00403	.00053	.54368	2.610-2.680	2.645±0.020	
Granite/granodiorite a	46	.00005- .04440	.00095	.81462	2.550-2.710	2.626±0.029	
Granite/granodiorite b	33		.00038	.59976			2.66 1)
Granite/granodiorite c	13		.00935	.25629			
Gabbro	5	.00059- .00942	.00144	.42063	2.970-3.120	3.078±0.055	
GÅL'DENVARRI FORMATION							
Amphibolite	26	.00019- .14160	.00123	.69019	2.800-3.110	2.946±0.076	2.95
MASI FORMATION							
Quartzite a	49	.00001- .30940	.00050	1.17017	2.520-2.840	2.645±0.072	
Quartzite b	36		.00012	.47394			2.65 1)
Quartzite c	13		.02705	.66934			
ČAS'KEJAS FORMATION (NORTHERN PART)							
Amphibolite a (Meta-diabase/-tuff)	198	.00028-1.89913	.00454	.97020	2.640-3.390	2.963±0.098	
Amphibolite b (Meta-diabase/-tuff)	123		.00092	.15994			2.96
Amphibolite c (Meta-diabase/-tuff)	75		.06261	.59266			
Greenstone a	65	.00026- .33831	.00417	.98961	2.650-3.180	2.876±0.116	
Greenstone b	42		.00083	.19689			2.86
Greenstone c	23		.07946	.40088			
Albite-felsite a	22	.00012- .44715	.00236	1.19546	2.560-3.060	2.784±0.114	
Albite-felsite b	14		.00036	.31202			
Albite-felsite c	8		.06312	.74482			
Pelitic rocks a	25	.00015- .41287	.00455	1.14591	2.670-3.070	2.828±0.100	
Pelitic rocks b	15	.00064- .27516					
Pelitic rocks c	10	.08650- .66398					
Carbonate rocks	21	.00003- .11646	.00044	.92388	2.670-2.920	2.793±0.063	
BIK'KAČÅKKA FORMATION AND ČAS'KEJAS FM.(EAST)							
Mudstone a	41	.00008- .41325	.00133	.94365	2.480-3.080	2.743±0.101	
Mudstone b	32		.00047	.35721			2.76
Mudstone c	9		.05390	.54239			

ČAS'KEJAS FORMATION (SOUTHERN PART)								
Amphibolite a (Meta-diabase/-tuff)	49	.00055- .24772	.00316	.91168	2.840-3.070	3.010±0.053		
Amphibolite b (Meta-diabase/-tuff)	36		.00091	.08550			2.98	
Amphibolite c (Meta-diabase/-tuff)	13		.09905	.25552				
Mica schist	11	.00003- .00314	.00025	.62334	2.510-2.770	2.681±0.086		
AV'ŽI FORMATION								
Amphibolite	8	.00043- .14722	.01808	.90472	2.790-3.030	2.921±0.078	2.92	
NJALLAJÅKKA FORMATION								
Amphibolite a	33	.00014- .67359	.00577	1.02183	2.700-3.190	2.931±0.116		
Amphibolite b	17		.00072	.25417			2.94	
Amphibolite c	16		.05312	.53094				
Mica schist	7	.00008- .05955	.00080	.82111	2.560-2.880	2.764±0.093		
Carbonate rocks	6	.00009- .03501	.00093	1.01918	2.670-2.840	2.778±0.053		
SUOLUVUOBMI FORMATION								
Amphibolite a	93	.00009- .23014	.00193	.73878	2.640-3.260	2.958±0.110		
Amphibolite b	69		.00077	.19027			2.95	
Amphibolite c	24		.02698	.49424				
Albite-felsite	35	.00002- .10669	.00024	.68367	2.560-2.820	2.665±0.058		
Mica schist	50	.00004- .13675	.00045	.52559	2.430-2.890	2.727±0.078	2.72	
Quartzite, sandstone	15	.00004- .00052	.00019	.27609	2.600-2.920	2.682±0.074		
LIK'ČA FORMATION								
Greenstone a	83	.00006- .36156	.00242	.85113	2.700-3.070	2.882±0.090		
Greenstone b	60		.00078	.22931			2.88	
Greenstone c	23		.04648	.44431				
Albite-felsite	7	.00013- .17673	.00080	1.03244	2.550-2.950	2.682±0.130		
Sandstone	10	.00003- .23167	.00043	1.34363	2.600-2.830	2.661±0.063		
Pelitic rocks	11	.00019- .31178	.00263	.97638	2.530-3.180	2.788±0.147		
ČARAVARRI FORMATION								
Sandstone	12	.00007- .02321	.00037	.69150	2.620-2.790	2.680±0.050	2.68	1)
ALBITE DIABASE	26	.00021- .38481	.02594	.89402	2.650-3.140	2.918±0.117	2.90	
CALEDONIAN NAPPES AND DIVIDAL GROUP								
Arkose and sandstone	27	.00001- .00072	.00010	.40864	2.560-2.800	2.642±0.046		

density also occur. The supracrustal rocks within the Kautokeino Greenstone Belt show broad variations in the density distribution diagrams. The amphibolites and diabases have a dominating high density component. The density of the mafic volcanites depends on metamorphic grade. Along the central axis of the belt greenstones have a lower density than the equivalent higher grade amphibolites at the margins of the belt. The quartzites in the Masi Formation and the sandstones in the Čaravarri Formation show the lowest densities within the supracrustals.

With regard to the magnetic properties all distributions cover wide ranges. The highest susceptibility is found in the supracrustal rocks, especially the mafic ones, i.e. greenstones, mafic tuff/tuffites, amphibolites and diabases. The bimodal distribution for the supracrustal rocks is clearly seen. The diagrams show one low paramagnetic component and one high ferromagnetic, the latter mostly caused by magnetite (usually more than 1%). This bimodal distribution of the supracrustal rocks causes the banded pattern of the Kautokeino Greenstone Belt seen on the aeromagnetic map in Plate 2. The lowest susceptibility values are found in psammitic rocks due to a low content of paramagnetic silicates.

Similar petrophysical data have been published from other Precambrian shield areas (Henkel 1976, Gibb & Thomas 1980, Subrahmanyam & Verma 1982).

Aeromagnetic interpretations

The aeromagnetic measurements in this area were carried out in two periods. In 1959-62, measurements with a profile spacing of one kilometre and flight of altitude 150m were made. Printed maps were published in the scale of 1:100,000 (Nor. geol. unders. 1981a,b,c,d). Maps in the scale of 1:50,000 have been digitised into 500·500m grid cells to generate the coloured map shown in Plate 2.

During 1975-84 some areas were measured with a profile spacing of 250m and a flight altitude of 50m (Plate 2, Håbrekke 1975, 1979a,b, 1980a,b, 1981, 1983, 1984). These measurements are much more detailed than the former and are therefore used in the interpretations. Because their rights are restricted the original measurements are not shown here.

The aeromagnetic interpretations made here are based on methods developed at the Geological Survey of Sweden (Henkel 1975,1979, 1984,1985). The whole of northern Fennoscandia is now interpreted using this method by the Nordkalott Project, a collaboration project by the Geological Surveys of Finland, Norway and Sweden.

The interpretations were originally made on maps at the scale of 1:100,000 and the results are shown in a reduced scale in Plates 7 and 6. Plate 7 showns magnetic dislocations while Plate 6 depicts magnetic patterns, contacts and magnetization levels. Magnetic dislocation embraces the following features:

1. Linear discordances in the anomaly pattern.
2. Displacement of reference structures.
3. Linear magnetic gradients.
4. Discordant linear minima.

The three first characteristic features of magnetic dislocation are effects arising from faulting. The last one is caused by the oxidation of magnetite into hematite along fracture zones (Henkel & Guzman 1977). This feature is usually seen only on the low-altitude measurements. The interpretation reveals faults and fractures within the survey area that are indicated by their magnetic effects. The zones must be of a certain minimal magnitude (i.e. width, length and displacement and/or depth of weathering) to appear on the magnetic anomaly picture. The smallest detectable displacement is 100-200m on the low-altitude measurements.

As seen from the direction frequency spectrum in Plate 7 a very distinct pattern of dislocations emerges from the data with dominating directions N155°E, N5°E and N40°E. Generally the NNW-SSE trend seems to be the oldest. However, during separate periods, block displacement in several directions may have reactivated the same dislocation systems, and today only the accumulated effect is visible. This hampers the interpretation of the relative ages of the dislocation systems.

Many of the magnetic dislocations can readily be related to geological events. The NE-SW trend, most prominent in the northeastern and southwestern part of Plate 7 is related to faults and fault-systems. Intrusions of albite diabases commonly occur along the same systems. On the interpretation maps of the Nordkalott Project the same magnetic dislocation lineament system can be followed to the south into the Norrbotten area in northern Sweden. In the Masi area late-Quaternary faults cross-cutting the glacial overburden are governed by this NE-SW-trending dislocation system (Olesen 1985).

The best example of a N-S-trending dislocation is the fault-zone east of Čaravarri (Plate 1), which seems to have a vertical displacement of about 4-5km. Characteristic for many of the N-S and NW-SE dislocation trend is a strong alteration of the country rocks (albitization and carbonatization).

An interpretation map of magnetic pattern and contacts is shown in Plate 6. Magnetic patterns are identified by the following criteria (Henkel 1984,1985).

1. Banded pattern - representing continuous and parallel magnetic anomalies. The width of bands indicate width of the magnetic rocks.
2. Dyke-like pattern - representing continuous and discordant magnetic anomalies.
3. Irregular anomaly pattern - areas lacking any of the previously mentioned features.

In areas which have a banded magnetic pattern, steep to vertical dipping connections (bands) are distinguished from those with flat or gentle dips.

Magnetic contacts are defined as the location of changes in the magnetic pattern or the level of magnetization. For areas with a banded pattern two levels of magnetization are identified for both the flat-lying and the steeply dipping connections, and for areas with an irregular pattern three levels are discerned.

The analysis makes it possible to separate areas of supracrustal rocks from areas of plutonic rocks. The supracrustal rocks have a banded pattern due to a bimodal distribution of the susceptibility values (Plate 8). The banding represents the primary layering of these rocks. The irregular pattern in the gneisses and plutonic rocks is partly caused by the less distinct bimodal distribution of the susceptibility values (Plate 8) and partly by the more diffuse structurs in these rocks.

On the interpretation map, patterns of the regional distribution of the three mentioned rock types can be seen, illustrating the close relationship in the deformation between the gneiss complex and the surrounding greenstone belt. This situation is for instance seen in the Čier'te area where the volcanites in the Njallajåkka Formation describe a syncline around a basement dome (Fareth et. al. 1977). In the greenstone belt, a banded pattern can be seen wrapping around oval areas with an irregular pattern and low magnetization. These relationships are due to either domeformed areas where the Masi Formation crops out as in the Addjit and Spalloai'vi anticlines, or younger granitoid diapirs as the quartz monzonite in the Riednjajav'ri area and the granodiorite at Lavvoai'vi. Another example of the latter, not so pronounced on aeromagnetic maps, is the granodiorite on Værd'naš.

The distribution of the sedimentary Bik'kacåkka and Čaravarri Formations is seen from Plate 6. However, their exact contacts to the surrounding volcanites are not so distinct because the rocks are intruded by younger diabases. Further, there is a marked difference in the magnetic levels between the greenstone east and west of the Čaravarri Formation even though these are correlated on geological grounds.

Another striking feature seen from Plate 6 is the sudden change in the magnetic pattern from NNW-SSE-trending structures in the central part of the Kautokeino Greenstone Belt to NE-SW-trending to the northeast. From Plate 6 alone this could be interpreted as if the NE-SW structures are transected by the NNW-SSE set. From field observations it is clear that the prominent NE-SW-trending pattern is due to younger albite diabases that are partly related to faulting (see Plate 7) and partly controlled by older structures in the rocks (i.e. layering and foliation). It is not possible to find any important break between the two areas of different magnetic pattern on either geological or detailed geophysical grounds. The NNW-SSE-trending pattern east of Lavvoai'vi (Plate 6 and 1) is caused by the same type of diabases.

Gravimetric interpretations

A regional gravity survey was carried out during the years 1980-1985 (Gellein 1985). The measurements are made along profiles at 5-10km intervals with c. one km between the gravity stations. Special areas are measured in more detail with one gravity station per $1km^2$. The anomalies are terrain-corrected and compiled to Bouguer anomaly maps, made with an Applicon ink jet plotter (Plate 3).

Model calculations have been carried out along four E-W-trending profiles (Plate 9). The basic models used in the computer program (Lindberg 1982) are 2 ½D bodies, i.e. bodies of polygonal cross-section with the tails cut off in the strike direction.

The densities used in the gravity calculation are shown in Table 1. We have taken into account that most of the rock types and units are not 'pure' but consist of a mixture of different rocks. For the gneiss complexes, the Masi Formation and the Čaravarri Formation we have used a mean density of $2.67 \cdot 10^3 kg/m^3$ rather than the calculated values. This is done mainly because of the computer facilities. The density contrast between these units is very small (within $0.03 \cdot 10^3 kg/m^3$).

In the profiles B and C the gravimetric field is obviously composed of a long-wavelength regional field and a short-wavelength local field. Fig. 1 shows profile C-C' (see Plate 3) and illustrates how this regional field is thought to be the result of culminations in the basement. The acid gneiss complexes are thought to be underlain by intermediate gneisses with a density of c. $2.80 \cdot 10^3 kg/m^3$. Similar layered basement gneisses are found in northern Sweden (Lindroos & Henkel 1978, Lind 1985) and in the Lofoten

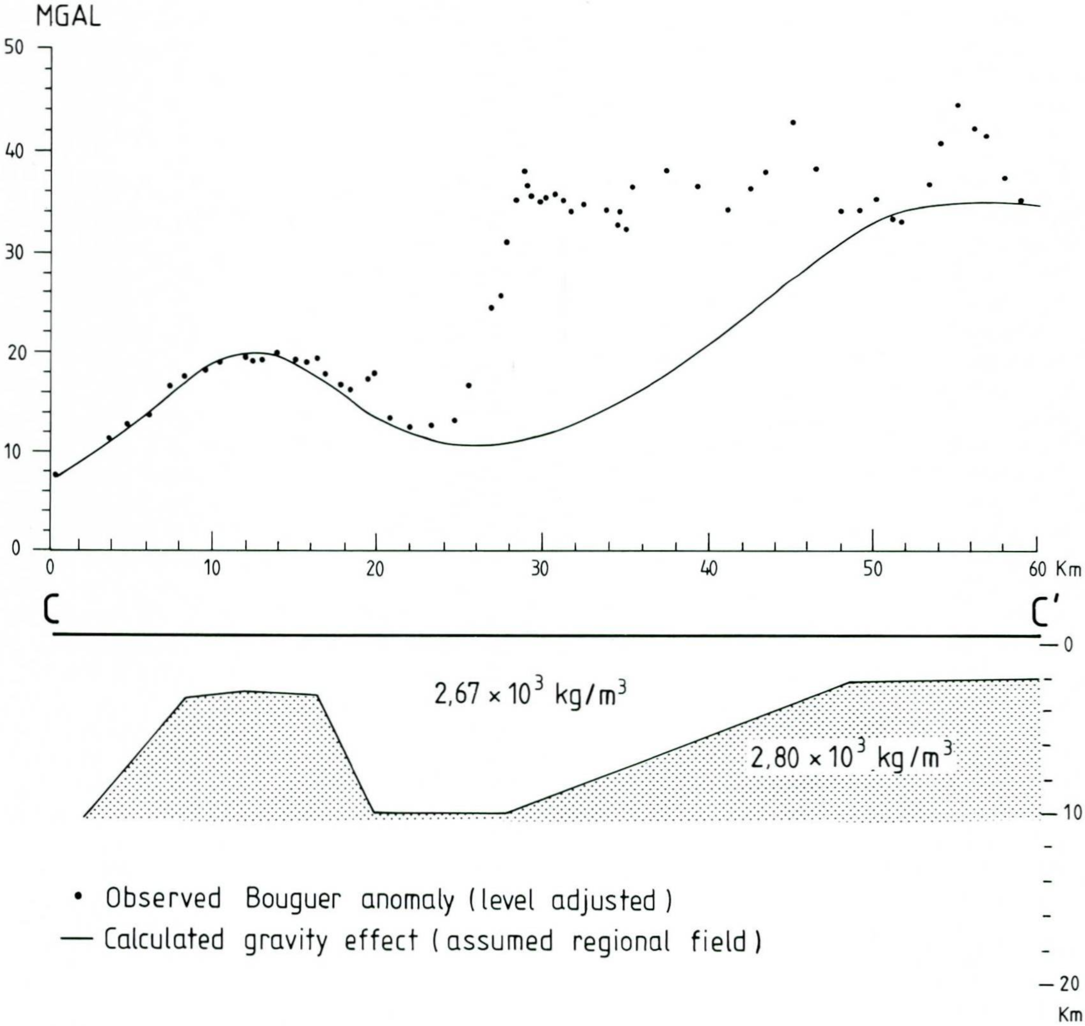

Fig. 1. Assumed regional gravity field of profile C-C'. Two culminations in a layered acid/intermediate basement complex explain the long wavelength regional field. Shaded area indicates intermediate basement.

area (Svela 1971). On Finnmarksvidda this layered basement is interpreted to form two large culminations with amplitudes of 5-7km in the Rai'sædno and Jer'gul Gneiss Complexes. In the latter only the western flank of the culmination is visible on this profile.

The central area, the Kautokeino Greenstone Belt, consists of alternating high and low gravimetric anomalies of short wavelengths. When compared with the geological map (Plate 1) it can be seen that the gravimetric lows mainly correspond to quartzites and sandstones in the Addjit anticline, the Čaravarri Formation and the Masi Formation, while the gravity highs mainly correspond to the basic volcanites in the Čas'kejas. Lik'ča and Gål'denvarri Formations. The largest gravity highs are interpreted as synclinoria of strongly folded and/or faulted amphibolites with depths of up to 6km.

From Plate 3 and 6 it can be seen that the large volume of mafic volcanics in the Kautokeino Greenstone Belt is deposited along NNW-SSE-trending axes, which are thought to be the direction of the rifting. The flat-lying thin sequences in the Masi area (Plate 1 and 6) are deposited at the margins of the rift. This is supported by the higher portion of sediments in this area.

More detailed interpretations are given in profiles A - D in Plate 9. The western part of profile A-A' is dominated by a synclinorium of amphibolites from the Čas'kejas Formation. The Biedjuvaggi Cu-Au mine (Hagen 1982) is situated in the central part of this synclinorium. East of this is an anticlinal structure which is thought to be the continuation of the anticline at Stuorajav'ri and Addjit on profiles B and C respectively. There is also a prominent gravity low caused by the Čaravarri Formation. The mudstone underlying the Čaravarri Formation is interpreted to have a depth of about 4-5km. Most probably the Čaravarri Formation also has the same depth. The gravity measurements do not allow the presence any greenstones below the Čaravarri Formation.

The easternmost gravimetric low is caused by an anticlinal structure of the Masi Formation (Plate 1). A magnetic anomaly caused by a deep-seated body is related to the same structure (Plate 2), and is interpreted as a sill-like intrusion of albite diabase, a relation that is generally found elsewhere in the Masi area (Solli 1983).

Profile B-B' has much in common with the former except that the supracrustal rocks are much thinner. At Stuorajav'ri there is only a thin sequence (100-300m) of metavolcanic rocks overlying the dome-shaped body of gneisses and quartzites. The western edge of the greenstone belt is interpreted to be strongly overfolded by the Rai'sædno Gneiss Complex. This interpretation is also supported from the aeromagnetic data (Plate 2) indicating a western dip of the basement/greenstone belt boundary. The easternmost gravity peak is shown on the profile to be caused only by the Gål'denvarri Formation, but it may also be an effect from basic intrusions.

Profile C-C' depicts the fault at Kautokeino. The amphibolites east of this which locally are named the Av'zi Formation (Olsen & Nilsen 1985) have a slightly lower density ($2.92 \cdot 10^3$kg/m^3) than the other amphibolites in the area (Table 1). The reason for this is partly the alteration (albitization) and carbonatzation. Small variations in the gravity field above the Rai's-ædno Gneiss Complex may be explained by lenses of amphibolites in the gneisses.

The southernmost profile (D-D') crosses the gravity high of the Riednjajav'ri area which is the most prominent gravimetric anomaly in the Kautokeino Greenstone Belt (Plate 3). The geology of this area has been studied in detail by Sandstad & Olesen (1984) and Sindre & Olesen (1983) and it is obvious that the anomaly is caused by downfolded basic volcanic rocks. The western part of the profile is covered by a quartz monzonitic intrusion. Its distribution is also seen as an irregular magnetization pattern in Plates 2 and 6.

Note also that on this profile it is necessary to take into account the gravity effect from the amphibolite north of the quartz monzonite (dotted line in the gravity profile).

Combined interpretation of the regional geophysical data

Plate 5 shows a combination map with an aeromagnetic interpretation map laid upon the Bouguer gravity map. By combining these two maps a three-dimensional analysis of the greenstone belt can be made in a rather effective manner. The colours indicate the depth of mafic volcanic rocks with a scale green - yellow - red showing increasing depth. In addition the banded pattern from the aeromagnetic interpretation depict the structures of the greenstone belt at the surface.

From the map it is evident that the gravity highs are generally related to synclinal structures composed of isoclinally folded and steeply dipping supracrustals (see Plate 6). Rounded gravity lows can be attributed to areas with the magnetic pattern forming conformal rounded structures. These are readily interpreted as domes consisting of granitic rocks or quartzites. The domes typically occur within and close to the supracrustal belt. Two of these basement domes were not recognized previously; they are, however, covered by thin sequences of volcano-sedimentary rocks. These two structures are found in the Stourajav'ri area and south of Kautokeino. As seen from the interpretation in Plate 6 these two areas are occupied by flat-lying bands interpreted as supracrustals. The sequence is thought to make up the roof of the domes. The Stuorajav'ri dome is traversed by profile B-B' (Plate 9). Examples of synformal structures are found at Biedjuvaggi as mentioned earlier, between Kautokeino and Addjit and between Spalloai'vi and Riednjajav'ri. These 4-6km-deep structures are also visible on the gravity interpretations along profiles A-A', C-C' and D-D' respectively (Plate 9).

An alternative interpretation of the positive gravity anomalies could be contributions from deep-seated mafic intrusions. This seems unlikely because the steep to vertical magnetic banding forms structures coinciding with gravity anomalies.

It is of interest to note that the two largest positive gravity anomalies (Biedjuvaggi and Riednjajav'ri) are associated with Cu-Au occurences. Corresponding correlation between Cu deposits and gravity highs are also reported from greenstone belts in Canada and Finland (Agterberg et al. 1972, Gaal 1984). This relation may be explained by the larger volumes of mafic rocks to derive the ore solutions from.

Discussion and conclusions

The Kautokeino Greenstone Belt is interpreted as a synclinorium of volcano-sedimentary rocks situated between two basement culminations. The basement is thought to be layered with an upper granitic and a lower intermediate layer explaining the long-wavelength gravity anomalies in the area. Within the greenstone belt alternating short-wavelength gravity highs and lows are due to synclines and domes, respectively. These structures are explained by the following process. Supracrustal volcanosedimentary basins of the Kautokeino Greenstone Belt have developed by rifting (tectonic extension) of a layered acid - intermediate crust with accompanying mafic volcanism. Volcanic units and sedimentary beds laid down on the older basement were subsequently deformed and metamorphosed.

According to numerical models (Mareschal & West 1980) the temperature of the granitic crust rises when the sedimentary rocks subside, and rocks are softened enough so that gravitational slumping follows. This process caused by gravitational instability has also been simulated by centrifuged models (Ramberg 1981, Dixon & Summers 1983). Based on these models the subsidence will start where the volcanic sequence initially is thickest. The subsidence is accompanied by doming of the upper part of the acidic basement into the greenstone belt. Simultaneously, isoclinal and upright folding may result in additional thickening of the downsagging basins. The domes are consequently formed in areas with the thinnest volcano-sedimentary sequences.

The formation of the dense greenstone belt caused regional instability. To re-establish equilibrium the layered crust culminated on either side of the belt and formed the Rai'sædno and Jer'gul Gneiss Complexes. In this late stage the uplifted basement was exposed to erosion and the sediments were deposited in basins in the greenstone belt. This process may explain the formation of the Čaravarri Formation. It consists of sandstones and conglomerates derived from a granitic source (Holmsen et al. 1957, Siedlecka et al. 1985).

According to Mareschal & West (1980) strong differences in temperature gradient arise between the ascending and descending parts of the crust. This convection causes lateral variations in the geothermal gradient. The horizontal change in metamorphic facies from high grade at the margins of the Kautokeino Greenstone Belt to very low grade in the centre could be explained in this way.

The foliation within the main basins of the subsiding Kautokeino Greenstone Belt, as for example at Biedjuvaggi and Riednjajav'ri, is steep, caused by strong vertical extension and horizontal contraction. Such directed stresses would act to produce strong vertical foliation (Dixon & Summers 1983). Initially horizontal layering tends to become transposed into a vertical orientation subparallel to foliation.

It can be concluded that the proposed gravitational tectonic model will explain the observed main structures in the Kautokeino Greenstone Belt. It is not necessary to include compressional tectonics in the model.

The model described above concerning the development of the greenstone belt on older sialic granite-gneiss-basement is very similar to interpretations suggested for similar greenstone belts in Sweden, Canada and India (e.g. Lindroos & Henkel 1978, Gibb & Thomas 1980, Subrahmanyan & Verma 1982).

Acknowledgements

The gravity measurements and much of the petrophysical laboratory work have been performed by several colleagues in the Finnmark Programme and the Geophysical Department of the Geological Survey of Norway. A/S Prospektering permitted us to use the low-altitude aeromagnetic measurements financed by the company. A. Krill, M. Often, and A. Siedlecka have critically reviewed the manuscript. H. Henkel, J.S. Sandstad and A. Sindre have contributed with valuable discussions. To all these persons and institusions we express our sincere thanks. We also acknowledge D. Roberts for correcting the English text, T. Aune for typing the manuscript and B.I. Svendgård and T. Thoresen for preparing figures and plates.

References

Agterberg, F.P., Chung, C.F., Fabbri, A.G., Kelly, A.M. & Springer, J.S. 1972: Geomathematical evaluation of cop-

per and zinc potensial of Abitibi area, Ontario and Quebec. *Geol. Surv. Can.* Paper 71-46.
Bergh, S. & Torske, T. 1984: Vulkanske facies og avsetningsmiljø, Kvenvikgrønnsteinen i Alta, Nord-Norge. XVI Nordiska Geol. Vintermøtet. Stockholm 1984. Abstract.
Dixon, J.M. & Summers, J.M. 1983: Patterns of total and incremental strain in subsiding troughs; experimental centrifuged models of inter-diapir synclines. *Can. J. Earth Sci. 20*, 1843-1861.
Fareth, E., Gjelsvik, T & Lindahl, I. 1977: Cier'te. Beskrivelse til berggrunnsgeologisk kart 1733 II - 1:50 000. *Nor. geol. unders. 331*, 28pp.
Gaal, G. 1984: Evaluation of the mineral resource potensial of central Finnish Lapland by statistical analysis of geological, geochemical and geophysical data. *Geol. Surv. Finland*, Rep. Invest. 63, 69 pp.
Gellein, J. 1985: Gravimetrisk Bougueranomalikart, Finnmarksvidda, M 1:250 000. Unpubl. NGU report 85.179, 11 pp.
Gibb, R.A. & Thomas, M.D. 1980: Correlation of gravity anomalies with Yellowknife Supergroup rocks, North Arm, Great Slave Lake. *Can. J. Earth Sci. 17*, 1506-1516.
Hagen, R. 1982: The Bidjovagge Copper-Gold Deposits of western Finnmark, Norway. *Geol. Rundsch. 71*, 93-103.
Henkel, H., in Witschard, W. 1975: Description of the geological maps Fjällåsen NV,NO,SV,SO. *Sver. geol. unders. Af 17-20*, 97-125.
Henkel, H. 1976: Study of density and magnetic properties of rocks from Northern Sweden. - PAGEOPH 114/2.
Henkel, H. & Guzman, M. 1977: Magnetic features of fracture zones. *Geoexploration 15*, 173-181.
Henkel, H. 1979: Dislocation sets in northern Sweden. *Geol. För. Stockholm Förh. 100*, 271-278.
Henkel, H. 1984: Nordkalottprojektet - flymagnetisk tolkning i testområdet. Unpubl. SGU report 84.04, 22 pp.
Henkel, H. 1985: The North Calotte Projectreport on the aeromagnetic interpretation map. Abstract. XV Nordiska geofysikermøtet 15.-17. janueri 1985, Esbo, Finland.
Holmsen, P., Padget, P. & Pehkonen, E. 1957: The Precambrian geology of Vest-Finnmark, Northern Norway. *Nor. geol. unders. 201*, 106 pp.
Håbrekke, H. 1975: Magnetiske- og elektromagnetiske målinger fra helikopter over Čierte, Nordreisa, Troms og Kautokeino, Finnmark. Unpubl. NGU report 1271, 8 pp.
Håbrekke, H. 1979a: Radiometriske- og magnetiske målinger fra helikopter over Njallaav'zi, Nordreisa, Troms. Unpubl. NGU report 1430/2A, 9 pp.
Håbrekke, H. 1979b: Magnetiske-, elektromagnetiske-, radiometriske- og VLF-målinger fra helikopter over et område syd for Kautokeino, Finnmark. Unpubl. NGU report 1734, 12 pp.
Håbrekke, H. 1980a: Magnetiske-, elektromagnetiske-, VLF- og radiometriske målinger fra helikopter over Kautokeino syd, Kautokeino, Finnmark. Unpubl. NGU report 1782, 12 pp. Confidential.
Håbrekke, H. 1980b: Magnetiske-, elektromagnetiske-, VLF- og radiometriske målinger fra helikopter over Bidjovagge- området, Kautokeino, Finnmark. Unpubl. NGU report 1783, 12 pp. Confidential.
Håbrekke, H. 1981: Magnetiske-, elektromagnetiske-, VLF- og radiometriske målinger fra helikopter over Bidjovaggeområdet, Kautokeino, Finnmark. Unpubl. NGU report 1833, 12 pp. Confidential.
Håbrekke, H. 1983: Geofysiske målinger fra helikopter over et område rundt Masi, Kautokeino, Finnmark. Unpubl. NGU report 1902, 15 pp. Confidential.
Håbrekke, H. 1984: Geofysiske målinger fra helikopter over kartbladene Čarajav'ri og Jiesjav'ri, Finnmark. Unpubl. NGU report 1886/8, 15 pp.
Krill, A.K., Bergh, S., Lindahl, I., Mearns, E.W., Often, M., Olerud, S., Olesen, O., Sandstad, J.S., Siedlecka, A. & Solli, A. 1985: Rb-Sr, U-Pb, and Sm-Nd isotopic dates from Precambrian rocks of Finnmark, (this volume).
Lind, J. 1985: The Nordkalott project: Interpretations of the dome structure in the Gällivare-Vittangi area, Northern Sweden. XV Nordiska geofysikermøtet 15.-17. januari 1985, Esbo, Finland.
Lindberg, H. 1982: Användarbeskrivning för GAMMA, ett datorprogram för beräkning av gravimetriska eller magnetiska anomalier. Unpubl. SGU report FR8210/FM8219, 24 pp.
Lindroos, H. & Henkel, H. 1978: Regional geological and geophysical interpretation of precambrian structures in Northeastern Sweden. *Sver. geol. unders. C751*, 19 pp.
Mareschal, J.C. & West, G.F. 1980: A model for Archaean tectorism; Part 2, Numerical models of vertical tectonism in greenstone belts. *Can. J. Earth Sci. 17*, 60-71.
Norges geologiske undersøkelse 1981a: Aeromagnetisk kart 1733-1:100,000. Trondheim.
Norges geologiske undersøkelse 1981b: Aeromagnetisk kart 1832- 1:100,000. Trondheim.
Norges geologiske undersøkelse 1981c: Aeromagnetisk kart 1833- 1:100,000. Trondheim.
Norges geologiske undersøkelse 1981d: Aeromagnetisk kart 1932- 1:100,000. Trondheim.
Norges geologiske undersøkelse 1981e: Aeromagnetisk kart 1933- 1:100,000. Trondheim.
Olesen, O. 1985: Sen-/post-glaciale forkastninger ved Masi, Finnmark. Unpubl. NGU report 84.171, 27pp.
Olsen, K.I. 1984a: Roavvoai'vi, foreløpig berggrunnsgeologisk kart 1832 II - 1:50,000. *Nor. geol. unders.*
Olsen, K.I. 1984b: Šuvčaganvarri, foreløpig berggrunnsgeologisk kart 1932 III - 1:50,000. *Nor. geol. unders.*
Olsen, K.I. 1984c: Ur'devarri, foreløpig berggrunnsgeologisk kart 1832 III - 1:50,000. *Nor. geol. unders.*
Olsen, K.I. 1985: Lavvoai'vi, foreløpig berggrunnsgeologisk kart 1932 IV - 1:50,000. *Nor. geol. unders.*
Olsen, K. I. & Nilsen, K. 1985: Geology of the southern part of the Kautokeino Greenstone Belt. Rb-Sr geochronology and geochemistry of assosiated gneisses and late intrusions, (this volume).
Ramberg, H. 1981: Gravity, deformation and the earth's crust. 2nd ed. Academic Press, London 452 pp.
Sandstad, J.S. 1985: Mollejus. Foreløbig berggrunnsgeologisk kart 1833 IV - 1:50 000. *Nor. geol. unders.*
Sandstad, J.S. & Olesen, O. 1984: Kobber - gullmineraliseringer ved Riednjajavr'ri, Kautokeino. *In* "Et informasjonsmøte om Finnmarks geologi". M. Often (ed.). Unpubl. NGU report 84.095, 91-97.
Siedlecka, A., Iversen, E., Krill, A.G., Lieungh, B., Often, M., Sandstad, J.S. & Solli, A. 1985: Lithostratigraphy and correlation of the Archean and Early Proterozoic rocks of Finnmarksvidda and the Sørvaranger district, (this volume).
Sindre, A. & Olesen, O. 1983: Geologisk og geofysisk tolkning av en større tyngdeanomali ved Riednjajav'ri, Kautokeino. Unpubl. NGU report nr 1886/2, 20pp.
Solli, A. 1983: Precambrian stratigraphy in the Masi area, Southwestern Finnmark, Norway. *Nor. geol. unders. 380*, 97-105.
Solli, A. 1984a: Masi. Foreløbig berggrunnsgeologisk kart

1933 IV - 1:50 000. *Nor. geol. unders.*
Solli, A. 1984b: Čarajav'ri. Foreløbig berggrunnsgeologisk kart 1833 I - 1:50 000. *Nor. geol. unders.*
Subrahmanyam, C. & Verma, R.K. 1982: Gravity interpretations of the Dharwan greenstone-gneiss-granite terrain in the southern Indian Shield and its geological implications. *Tectonophysics 84*, 225-245.
Svela, P.T. 1971: *Gravimetriske undersøkelser av Lofoten Vesterålen området.* Unpubl. Cand.real.thesis, Univ. of Bergen, 131 pp.
Torske, T. 1978: En proterozoisk aulacogen i Nord-Norges grunnfjell. XIII Nordiske Geol. Vintermøtet, København. Abstract.

ERRATUM

Olesen & Solli, Plate 1
In the legend the terms
'Amphibolite (Gål'denvarri Fm.)'
and
'Quartzite (Masi Fm., etc.)'
should be interchanged.

Plate 1

Simplified geological map of the Kautokeino Greenstone Belt.

Modified from Fareth et al. 1977, Olsen 1984a, b, c, 1985, Sandstad 1985, Solli 1984a, b.

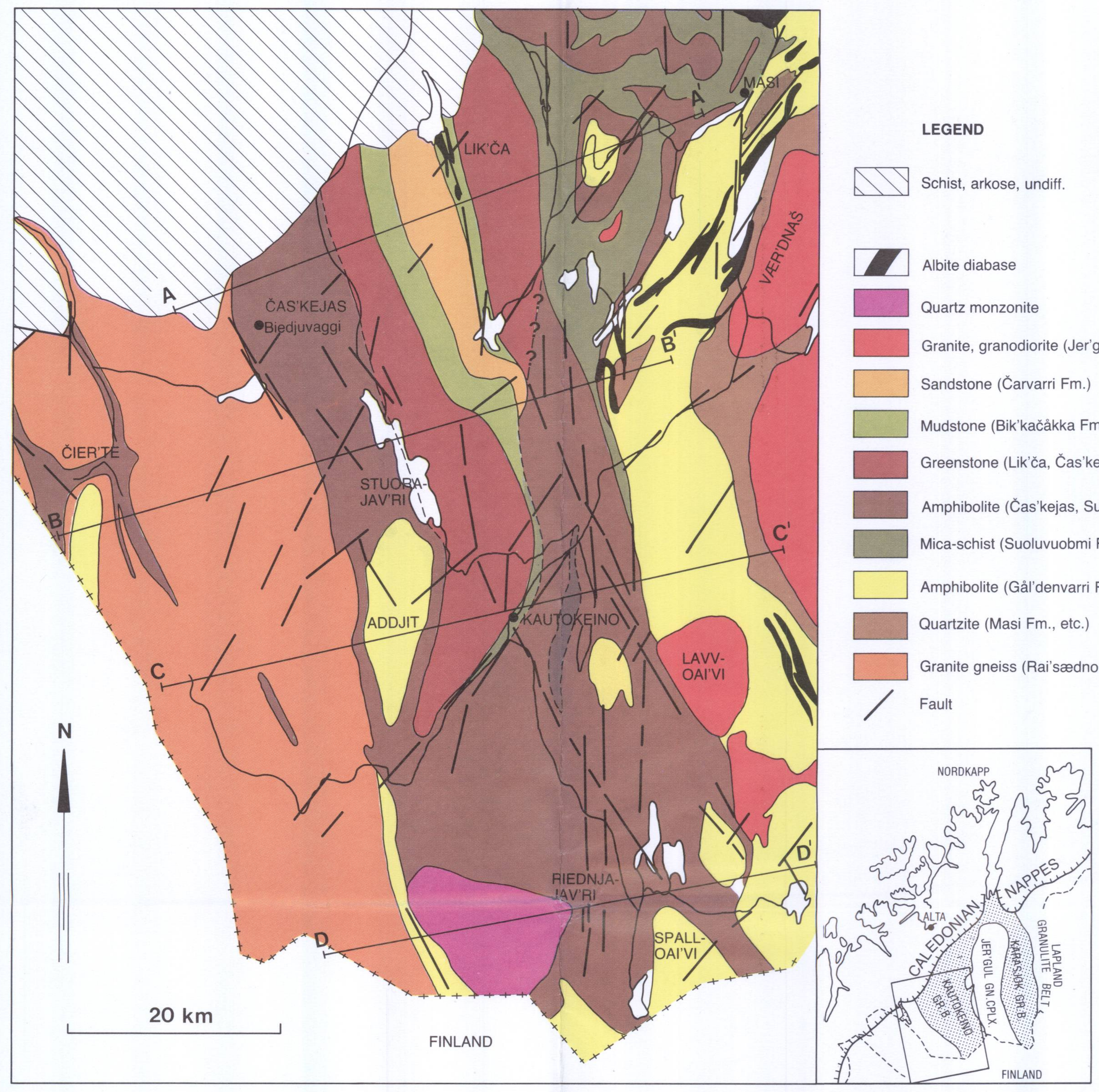

Plate 2

Aeromagnetic residual map.

Areas covered by low altitude measurements are shown by frames
Digitized from Nor. geol. unders. 1981a, b, c, a.

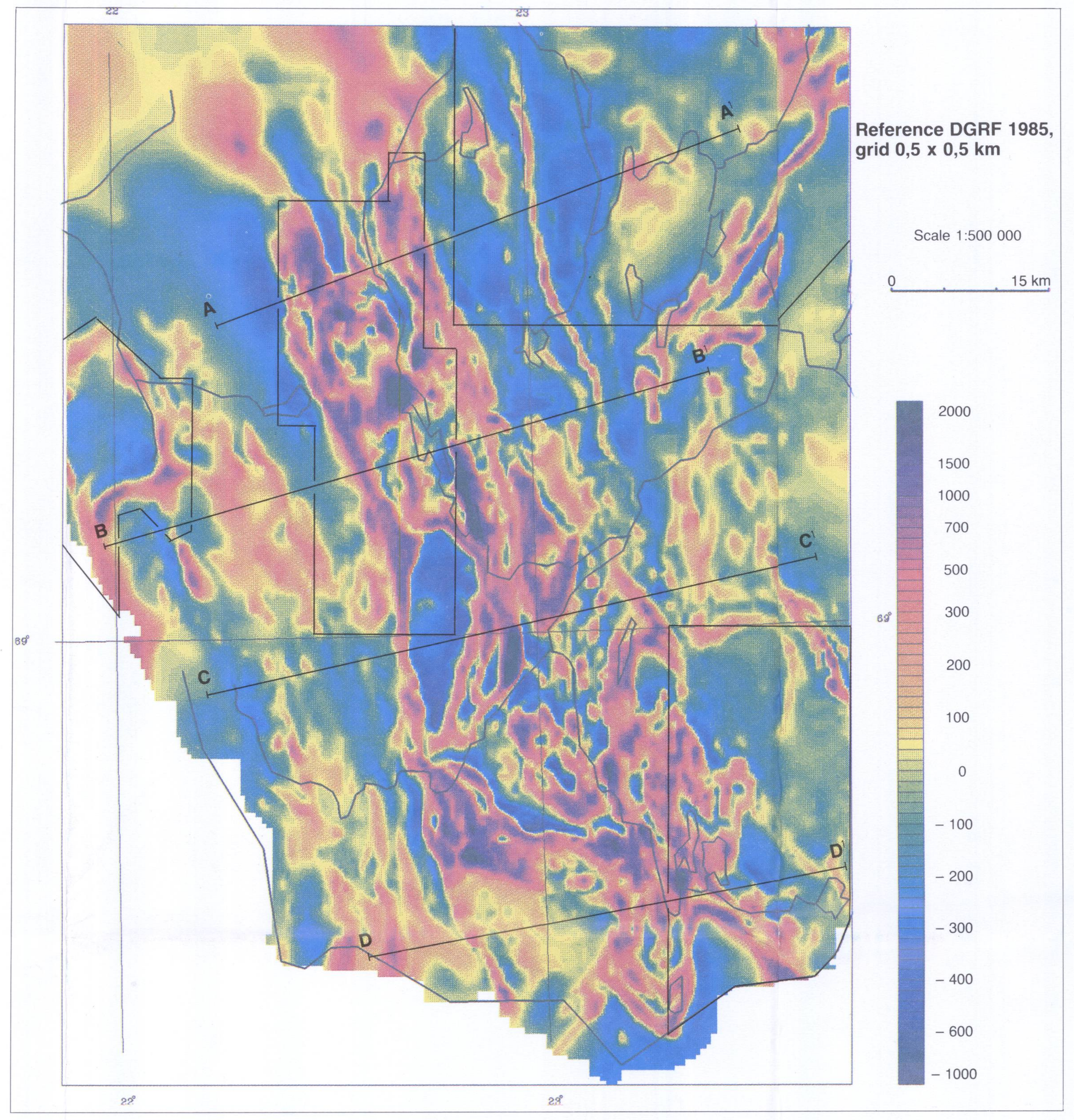

Plate 3

Bouguer gravity anomaly map.

After Gellein 1985.

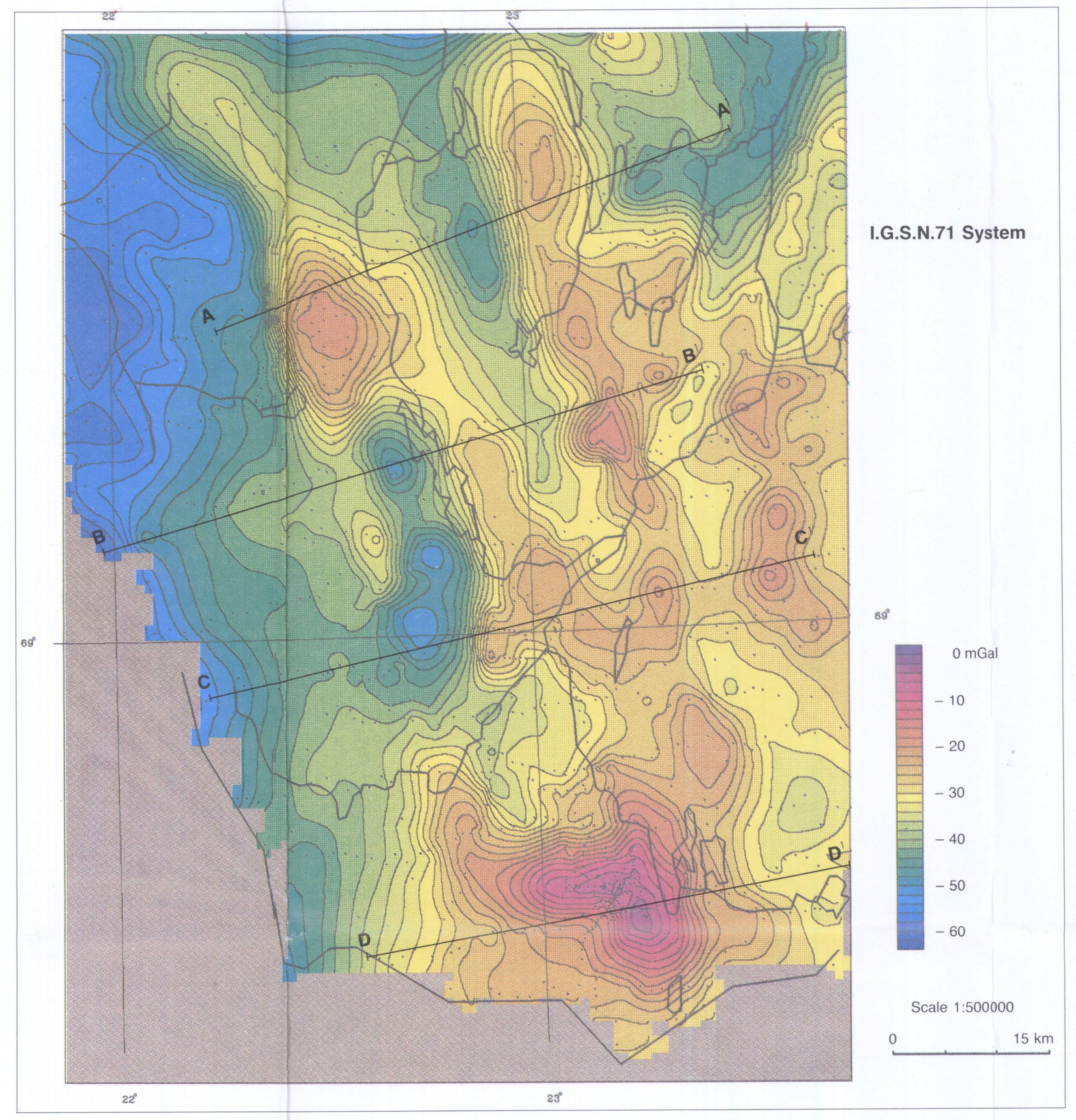

Plate 4

Density map. Data 1973–1984

The density values are indicated by 1x1 km coloured cells.
In cells with more than one sample an average value is shown.

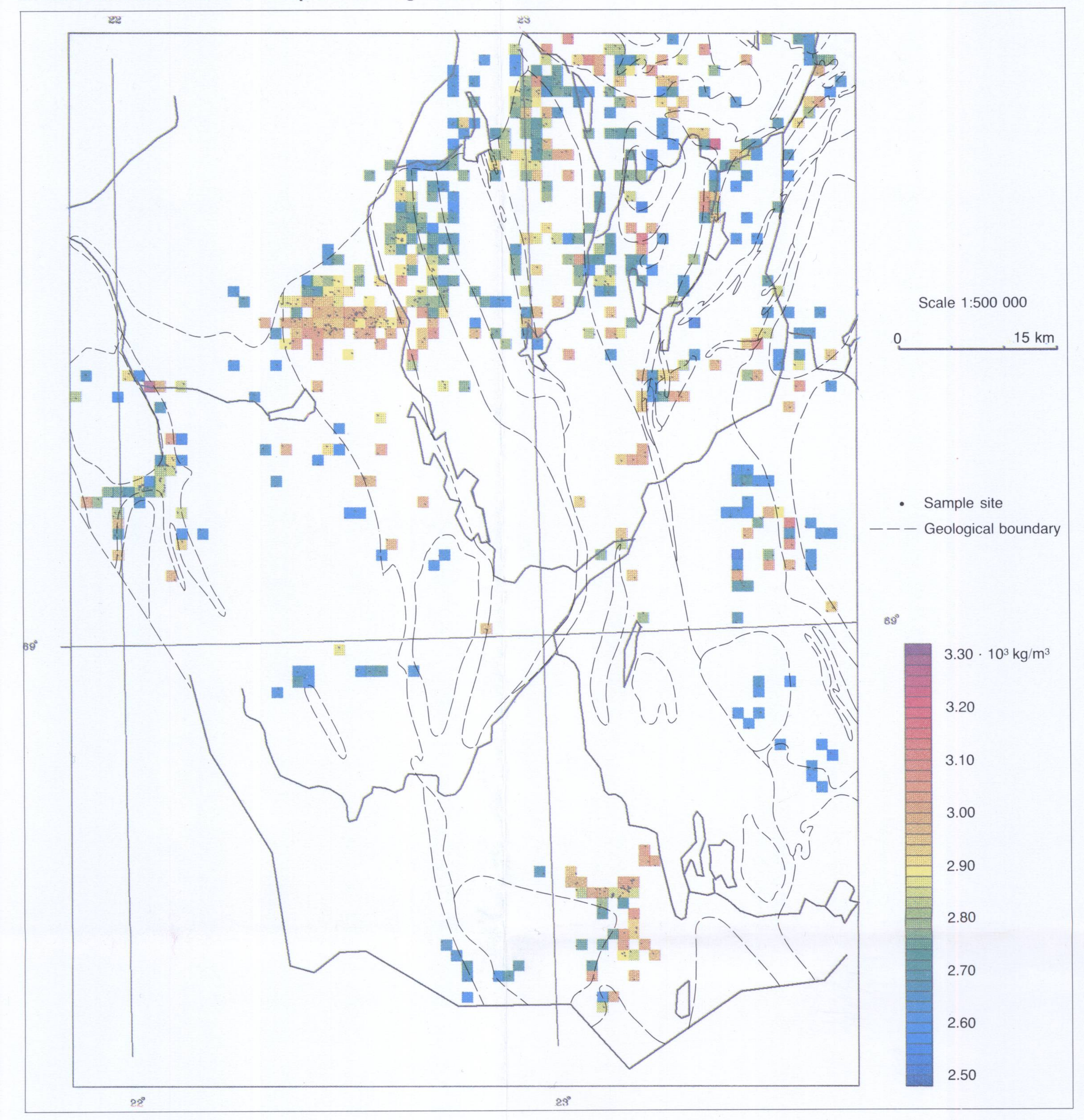

Plate 5

Combined magnetic structure and Bouguer anomaly map.

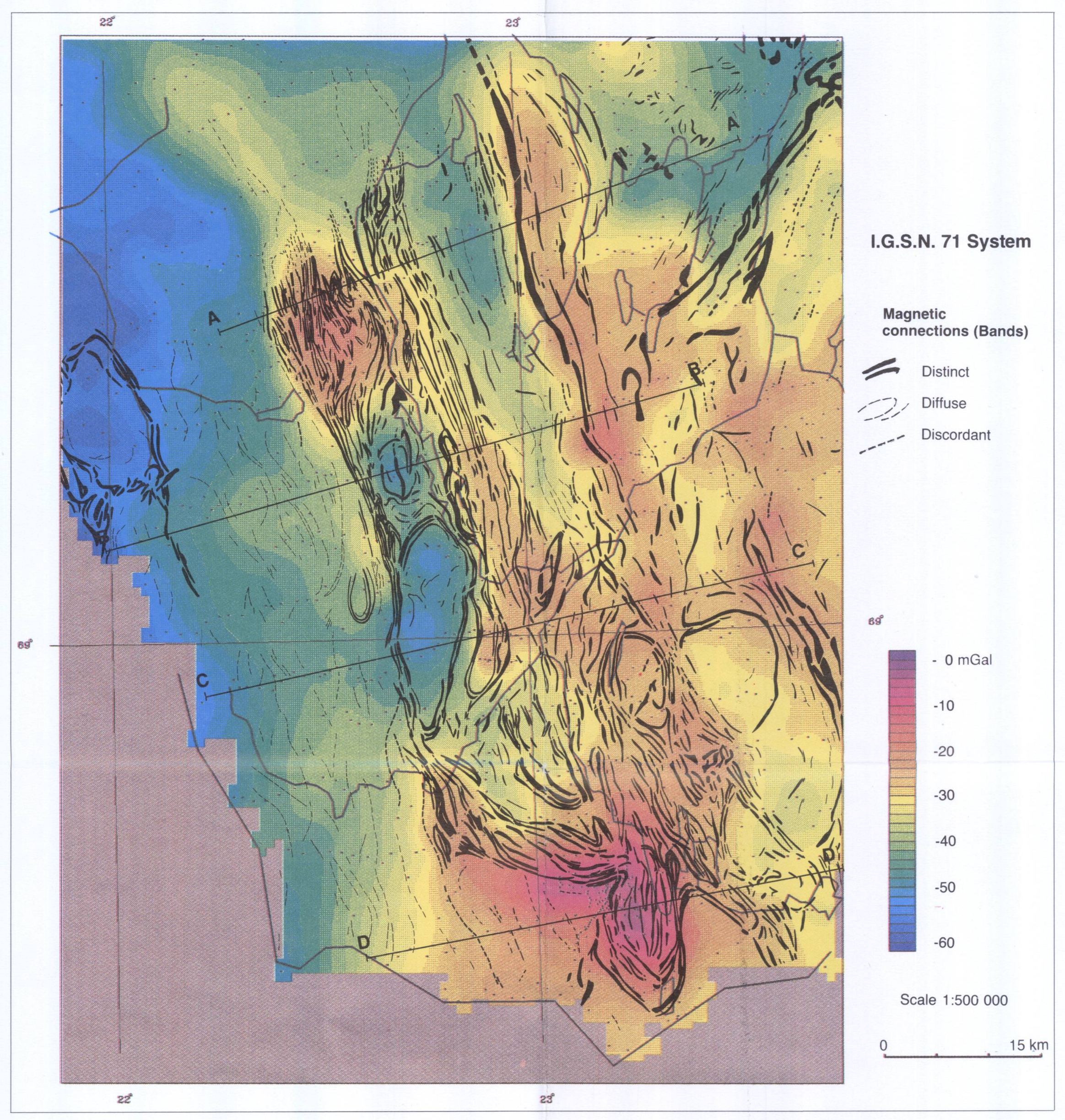

Plate 6

Magnetic structure map.

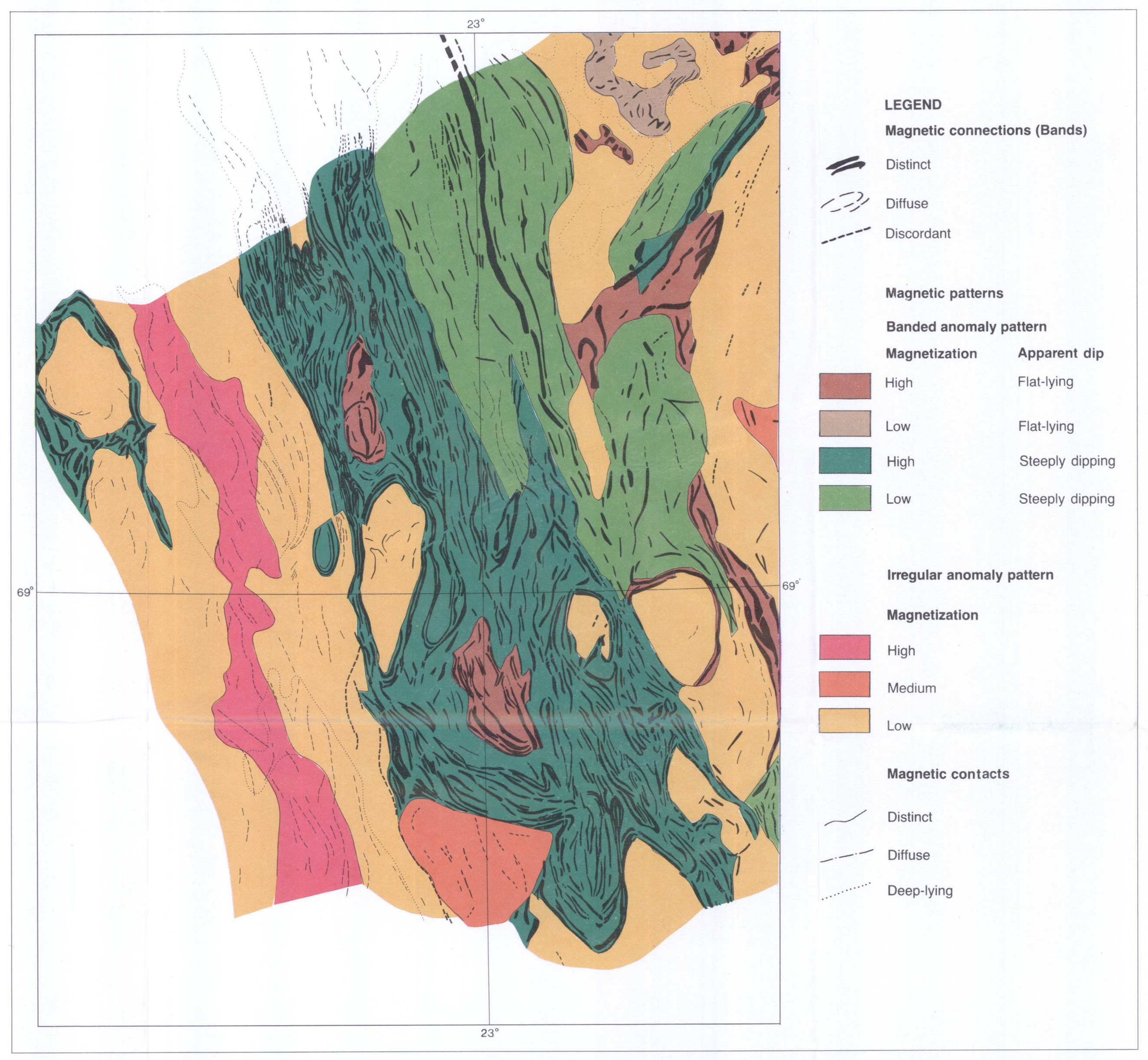

Plate 7

Magnetic dislocation map.

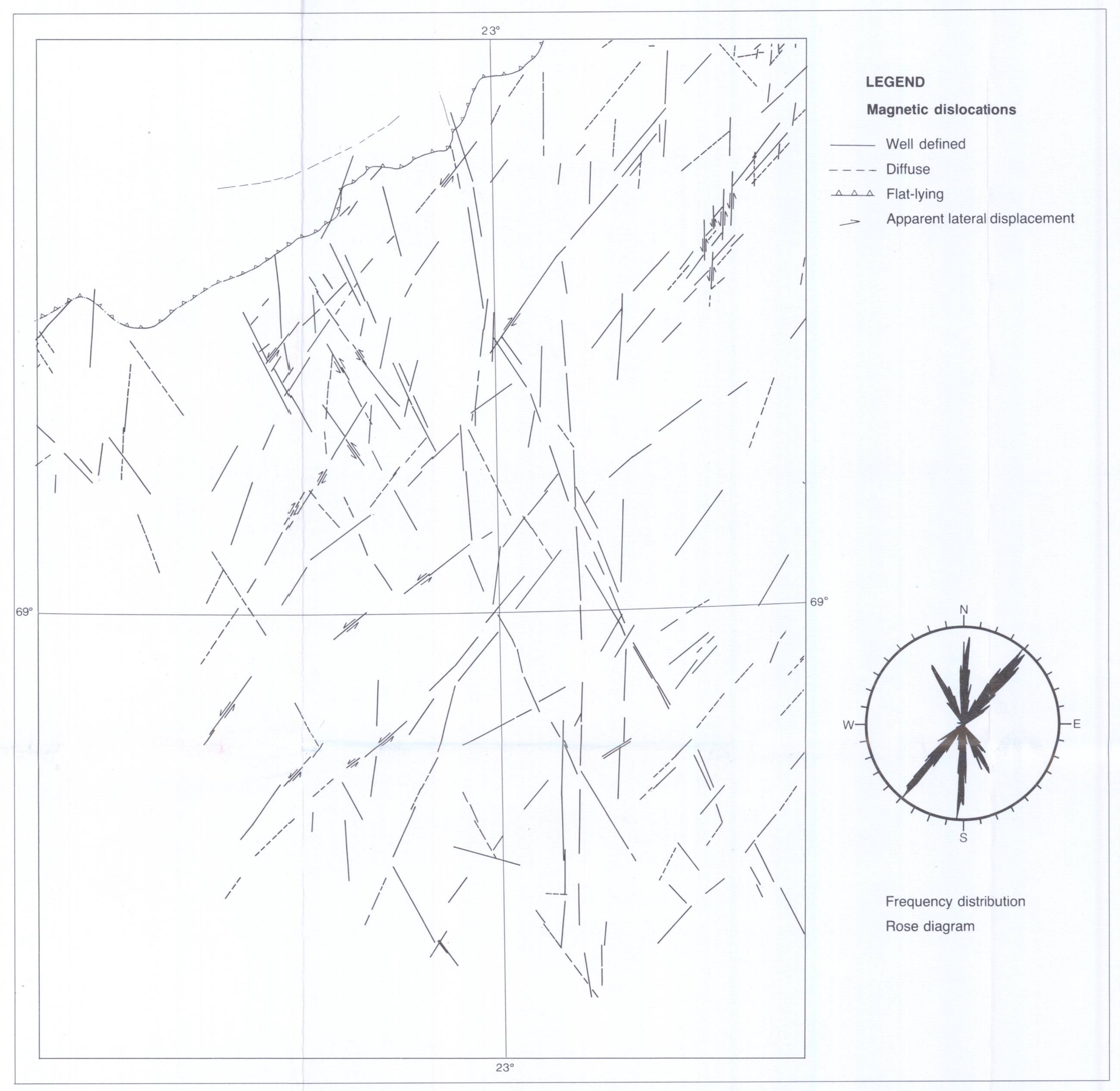

Plate 8

Density and susceptibility spectra of major rock types.

Density in 10³ kg/m³ and susceptibility in SI units.

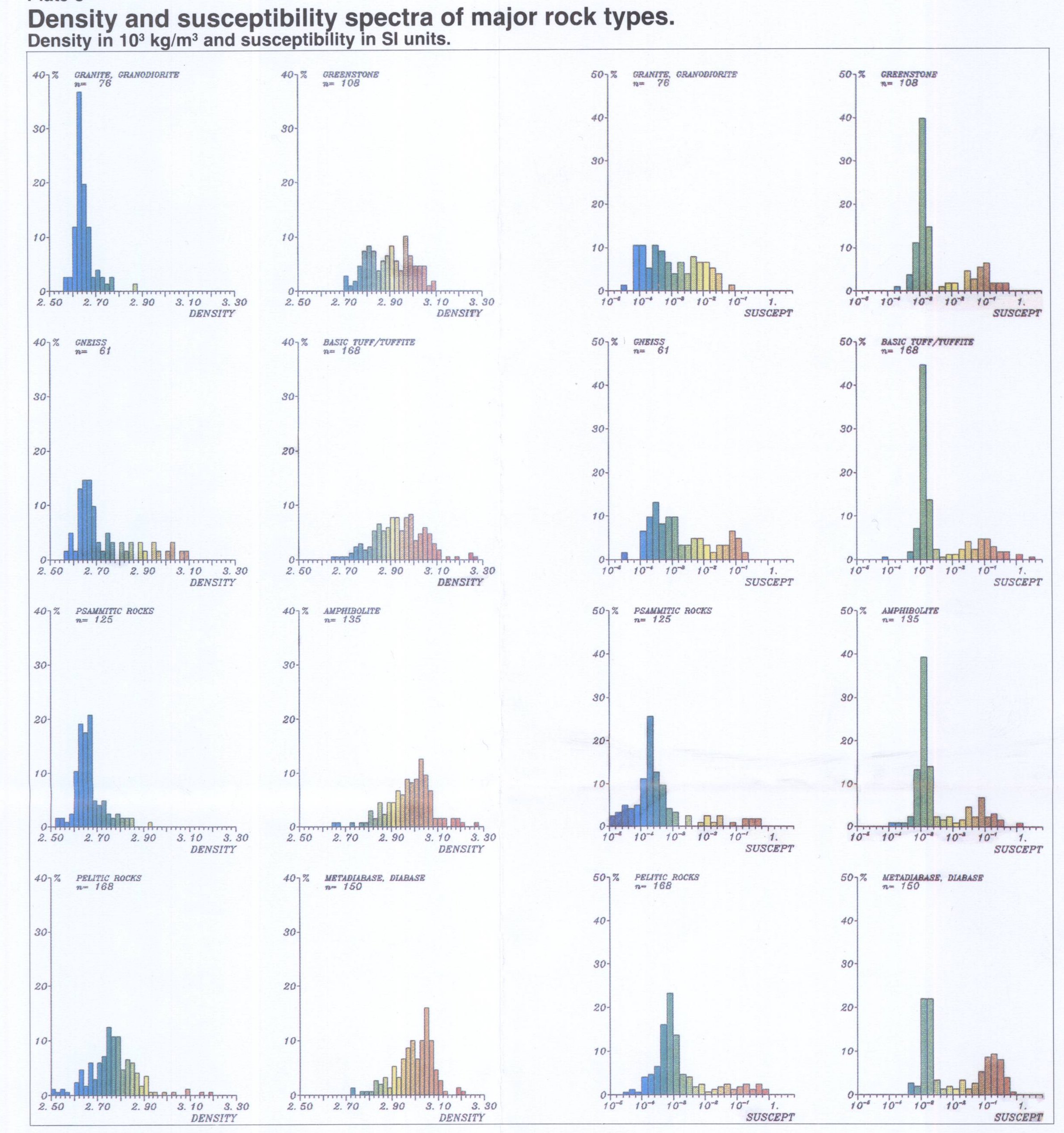

Plate 9

Four gravity sections across the Katuokeino Greenstone Belt.

Location of the profiles shown in Plates 1–5